Contents list available at CBIORE journal website

International Journal of Renewable Energy Development

Journal homepage: https://ijred.cbiore.id

Research Article

Radiator-type solar heating system with phase change material for residential thermal comfort

Kléber Janampa Quispe[a*], Octavio Cerón Balboa[a], Oswaldo Morales Morales[a], Julio Oré García[a], Hugo David Calderón Vilca[b]

[a]*Department of Mathematics and Physics, Faculty of Mining, Geology, and Civil Engineering, National University of San Cristóbal de Huamanga, Peru*

[b]*Software Engineering Department, Systems Engineering and Computer Science, National University of San Marcos, Peru*

Abstract. This paper presents the design, construction, and experimental thermal evaluation of a modular solar heating system that integrates heat collection, storage, and emission into a single compact unit. The prototype consists of a flat-plate solar air collector directly coupled to a radiator-type thermal storage module. The central innovation lies in the use of paraffin as a phase change material (PCM), encapsulated in twelve finned aluminum tubes. This configuration enables the storage unit to function simultaneously as a passive heat exchanger, ensuring a uniform and sustained release of the accumulated energy. Experimental results, obtained under a solar irradiance of 950 W/m², showed that the air temperature at the collector outlet exceeded 70 °C. During the discharge phase, the indoor ambient temperature remained within the thermal comfort range (20.5 °C–23.6 °C) for up to six hours, maintaining a 3–4 °C temperature difference relative to the outdoor environment. The latent heat storage capacity of the PCM effectively mitigated indoor temperature fluctuations, contributing to stable comfort conditions. In conclusion, the proposed system represents a significant innovation in passive solar energy technology, integrating the functions of collector, accumulator, and radiator into a low-cost, easily replicable modular device. Its constructive simplicity and thermal efficiency position it as a viable and sustainable solution for residential heating in cold climates and rural or hard-to-reach areas with limited energy access.

Keywords: Solar collector, phase change material, thermal comfort

Received: 5th May 2025; Revised:17th Oct 2025; Accepted: 28th November 2025; Available online: 18th Dec 2025

1. Introduction

The temperature inside a house can reach maximum or minimum values corresponding to the external climatic conditions. One of the influencing factors is the light envelope of modern dwellings, which have a low thermal capacity (Xiao, Wang, and Zhang 2009) that makes the temperature inside the house sensitive to the outside temperature, which makes the temperature and humidity conditions inside the house uncomfortable for its inhabitants and, in some cases, makes it necessary to use conventional energy sources to improve the internal climatic conditions of the house. Thermal comfort has a significant impact on the health and well-being of the inhabitants, and is related to the sociocultural situation, local adaptive behavior, the individual characteristics of the occupants, the external climate, including seasonal changes (Sansaniwal, Mathur, and Mathur 2022). It is therefore necessary to develop technologies that achieve thermal comfort inside a home, environmentally sustainable technologies that optimize the local solar energy potential. In the case of the southern highlands of Peru, they are located in the so-called "sun belt", which is characterized by a significant solar energy potential, by the distribution of solar radiation and by its global solar irradiation intensity throughout the year; its average daily solar intensity reaches high values between 6 to 7 kWh/m². The aforementioned factors influence in determining the efficiency of the applied solar technology (Maka and Alabid 2022) and mean that this technology has to be adapted to the characteristics of the site where it is to be applied.

The use of conventional energies, such as fossil fuels, for the thermal comfort of homes, contributes to the accelerated growth of greenhouse gas emissions and is therefore not environmentally sustainable; moreover, given the increase in price and scarcity of fossil fuels, technological research studies are oriented to the search for new alternative and renewable energy sources that offer sustainable energy solutions (Novas *et al.* 2021). In terms of sustainability, wind energy is one of the best sources of renewable energies (Akbari *et al.* 2022) and biomass is a traditional source of energy that is used to produce renewable energy in the form of fuels, heat and electricity (Shahzad *et al.* 2023). On the other hand, solar energy has the highest potential than the other sources and stands out as the most mature and widely accepted one (Novas *et al.* 2021).

Currently, several thermal comfort systems based on the use of solar energy have been developed for a dwelling, whether it is a family house, social housing or buildings (Godoy-Vaca *et al.* 2021). One approach is oriented to passive solar heat gain by taking advantage of the thermal properties of the building materials in the envelopes or enclosures, taking advantage of

* Corresponding author
Email: kleber.janampa@unsch.edu.pe (K. Janampa)

https://doi.org/10.61435/ijred.2026.61348
ISSN: 2252-4940/© 2026.The Author(s). Published by CBIORE

the orientation of the dwelling, etc. and optimizing it with the use of simulations using specialized software (Zhao, Liu, and Lu 2022), (Zhu *et al.* 2022) and incorporating thermal accumulators with phase change materials. Other heating systems are active systems that use solar energy collection systems by means of solar collectors that use air, water or hybrids with heat transfer fluids, which in turn incorporate heat pumps or fans that conduct the hot fluid into the interior of the house (Rabani, Bayera Madessa, and Nord 2021).

Phase change materials (PCMs) are used as a latent heat storage system. This is a very cost-effective and affordable method of conserving thermal energy for future use (Golovchak *et al.* 2023); they are capable of storing and releasing a large amount of energy. In the last decade, PCMs were widely used for thermal insulation in buildings and the studies conducted have been oriented on the applications of PCMs in specific fields, such as thermal comfort and energy efficiency of buildings (Zhang *et al.* 2023). Very few of them were oriented to PCMs contained in metallic tubes of rectangular section that at the same time fulfill the function of radiators; so, there is the need to investigate thermal comfort systems that have a thermal energy accumulator with PCM materials that works as a radiator. Nonetheless, applications with PCMs are usually constrained by the reliability, efficiency, cost and performance of the technology used, and significant improvement is still needed in characterizing the phase transition, thermal conductivity and material compatibility. In the case of inorganic PCMs, it is very important to take measures to avoid undercooling, supercooling and phase separation by adding nucleation agents.

In order to achieve the thermal comfort temperature of a dwelling, heating, ventilation and air conditioning (HVAC) energy systems are being developed. There are systems that use thermal energy storage (TES) systems with phase change materials (PCM) that are incorporated into walls or windows (Izadi *et al.* 2023) (Rahimpour *et al.* 2017), which improves the thermal inertia of the house with which a decrease in energy consumption and a significant improvement in the thermal comfort of the house is achieved (Uribe and Vera 2021). In active thermal storage systems, solar thermal accumulators of sensible heat or phase change are used, which are coupled to radiant floor or wall systems (Zhai *et al.* 2023); in turn, hybrid systems are developed that couple passive and active systems that improve the thermal performance of the house reducing its daily energy consumption by 44.16 % (Kong *et al.* 2020).

A problem of the populations of the high Andean areas, as well as the case of the Peruvian highlands of Ayacucho, is that they live exposed to extreme thermal conditions: low temperatures, frost and snowfall because in the construction of their homes they use inadequate materials to insulate, capture or store thermal energy, with the consequent loss of thermal energy through the building envelope (Molina Castillo 2016). In general, there is a lack of energy efficiency and bioclimatic heating criteria for their inhabitants and, in turn, there is a scarce accessible technological offer for thermal comfort.

The objective of this research work was to design and build a heating system that uses a single pass flat plate solar air collector as an energy collector with a radiator-type thermal energy accumulator, using kerosene as a phase change material and a pumping system to convey the hot air into the room. The system is modular and allows the installation of the necessary modules according to the energy requirement to acclimatize the interior of a house and achieve the required thermal comfort. The thermal evaluation of the system was made through a test case in the environmental conditions of the city of Ayacucho - Perú.

The importance of the proposed solar heating system is that it is oriented within the approach of sustainable technologies, by using renewable energy sources and contributing to the reduction of negative effects on the environment; it also constitutes an alternative to diversify the use of energy sources for heating. The optimization of the proposed heating system is conditioned by the seasonal and local nature of solar energy, which limits its performance due to the intermittent solar radiation. In order to give sustainability to the proposed technology, the design process takes into account the simplicity of its operation, its maneuverability and the accessibility to materials and manufacturing processes. The present work is oriented towards the seventh sustainable development goal (SDG) of the United Nations: ensure access to affordable, reliable, sustainable and modern energy for all (United Nations 2015).

Solar heating technologies are broadly categorized into passive and active systems. Passive systems leverage the thermal properties of building materials, as demonstrated by Kou *et al.* (2022, 2023) who utilized building envelopes and PCMs to store and release heat, significantly improving indoor temperatures and comfort. Similarly, Godoy *et al.* (2021) extended thermal comfort duration by incorporating PCM (RT25-RT30) into walls. Studies on multi-active façades (Gosztonyi *et al.*, 2017) and strategic shading and insulation (Yu, Yang, and Tian, 2008) further highlight passive strategies for energy savings. Bae *et al.* (2019) and Chi *et al.* (2021) contributed with systems using rock bed thermal storage and solar chimneys, respectively, operating without external power.

Active systems, which require external energy, have been extensively researched. Luo *et al.* (2017) and Plytaria et al. (2018, 2019) integrated solar energy with heat pumps and PCMs for building heating and underfloor systems, comparing performance with and without PCM. Athienitis (2007) combined geothermal heat pumps with solar design. System modeling and simulation are also prevalent; Shabgard *et al.* (2018) developed a thermal network model for a system with latent heat storage, while T. Li *et al.* (2023) and Zhai *et al.* (2023) used simulations and real-world applications to demonstrate performance improvements, with the latter achieving a 6 °C temperature increase in a residential building.

A key research focus is the integration of solar collectors with Phase Change Materials (PCMs) to counteract solar intermittency. Z. Wang *et al.* (2018, 2019, 2020) investigated collector-storage units using kerosene wax and micro heat pipe arrays, reporting efficiencies up to 67.5 % and sustained heat output. Sudhakar & Cheralathan (2021) developed a double-pass collector with encapsulated PCM, boosting efficiency from 31 % (without PCM) to 40 %. Koca *et al.* (2008) analyzed a combined collector/PCM system using $CaCl_2{\cdot}6H_2O$, and C. Li *et al.* (2019) developed tankless water heaters with composite PCMs. For medium temperatures, B. Li and Zhai (2017, 2018) developed a system with an erythritol-graphite composite PCM, achieving storage efficiencies around 40 %.

Enhancements in collector efficiency through PCM integration are well-documented. Badiei, Eslami, and Jafarpur (2020) reported an efficiency increase from 33 % to 46 %, while D. Wang *et al.* (2019) used dual-PCMs to increase efficiency by up to 24.1 %. Sakhaei & Valipour (2021) found that combining helically corrugated heat pipes with PCM reduced heat losses by 39.8 % and increased efficiency to 48.9 %. Algarni (2023) further optimized performance by integrating PCM with a heat sink, improving daily thermal efficiency by 6-8 %.

In summary, the state of the art demonstrates a clear trend towards hybrid and integrated systems that combine collection and storage. The use of PCMs is a prevalent and effective strategy for enhancing thermal performance, extending heat

discharge, and improving indoor thermal comfort, providing a solid foundation for the development of the compact collector-accumulator system presented in this work.

2. Heating System Design for Thermal Comfort

The designed solar heating system consists of three components: a solar air collector, a solar thermal energy storage system and an air flow system. The flat plate collector is the solar energy collection element of the system and performs the photothermal conversion of solar radiation, the thermal energy is stored in the storage system using industrial paraffin wax as phase change material (PCM). The storage system was assembled inside the collector on top of the collector plate, constituting a collector-accumulator unit, following the approach developed by Sudhakar that incorporates paraffin wax filled into spherical balls in the holes of the absorber plate (Sudhakar and Cheralathan 2021). Unlike heating systems that have an external thermal energy storage device (Z. Wang *et al.* 2018) (Z. Wang *et al.* 2019); the storage system proposed in this research, is of radiator-type where each unit has fins at one end to improve heat transfer and orient the thermal flow. The

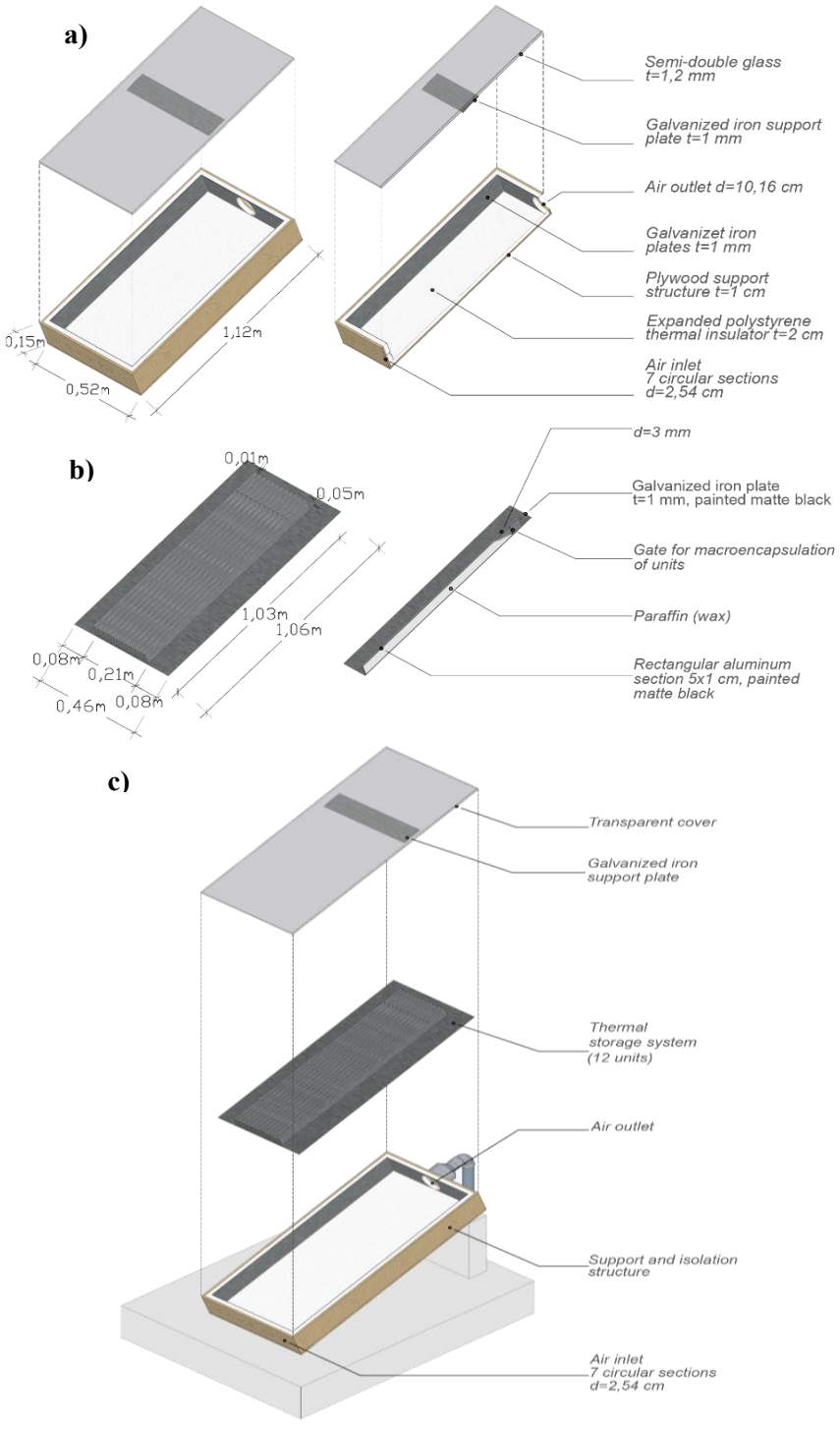

Fig. 1. Flat plate solar air collector-accumulator and the encapsulation of the paraffin-embedded storage units (a) Support and isolation structure (b) Thermal storage system (c) Components of the solar collector-accumulator

working medium in the whole system is air as a heat transferring fluid. When the collector is exposed to solar radiation, it starts the process of charging the storage system; when the solar radiation ceases, either during hours of low insolation or at night, the thermal discharge of the storage system begins, transferring it to the air. The hot air from the collector is conducted into the house by the air flow system, which forces and controls the movement of the hot air.

This study integrated theoretical design, material selection, prototype construction, and experimental validation to develop and evaluate an efficient solar heating system with Phase Change Material (PCM) storage, designed to provide thermal comfort in a dwelling under real solar conditions. The methodology was developed through several interconnected stages. First, during the system design and sizing phase, the main components—the solar air collector, the PCM thermal storage unit, and the airflow control system—were defined and characterized. In the experimental setup, sensors were installed to measure temperatures, solar irradiance, and airflow rate, and specific operating conditions were established to ensure test consistency and reproducibility. The experimental procedure comprised four consecutive phases: (i) airflow calibration and characterization, where airflow rates were determined for each fan speed; (ii) PCM charging, during which the system was exposed to solar radiation above 700 W/m^2 for approximately two hours while recording the temperatures of the collector, PCM, and air; (iii) PCM discharging, conducted without solar radiation to analyze the heat release from the PCM and its influence on indoor air temperature; and (iv) the comfort test, in which the heated air was introduced into the test chamber at the optimal fan speed, monitoring temperature variations at different points and heights. Finally, the thermal evaluation was performed using the collected data to determine the collector's performance parameters—such as the overall heat loss coefficient and the heat removal factor—and to analyze the system's behavior during the charging and discharging phases. The conception of the system design takes into account the simplicity of its operation, its maneuverability and accessibility to materials and manufacturing processes.

2.1 Heating system design

2.1.1 System components dimensioning procedure:

- The morphology and heating technique of the collector were dimensioned, determining the thermal and optical characteristics of the materials used.
- The main component, solar thermal storage, was dimensioned using the PCM macro encapsulation technique in 12 rectangular aluminum tube units, which also functions as a radiator.
- The air flow system, consisting of an exhaust fan (air pump), electronic air flow control and a hot air distributor, was characterized.

2.2.1 *System thermal evaluation procedure*

The following procedure is followed:

- The thermal performance of the flat collector is evaluated by experimentally determining the stagnation temperature of the collector plate, the inlet and outlet temperature of the air in the collector, with which the collector thermal performance curve is characterized, and the parameters that characterize its thermal performance, such as the removal factor and the overall loss coefficient, are determined. The data is obtained according to the thermal evaluation protocols for solar radiation conditions greater than 700 W/m^2 and external air flow velocity less than 2 m/s. The collector is fixedly oriented to the north and inclined 20° with respect to the horizontal.
- For the operation of the air flow control system, the speed and temperature change of the hot air that is extracted by the fan is characterized for four positions of the electronic system selector and for two different locations of the pump. This controls the level of hot air flow, according to the temperature requirement in relation to the optimum comfort temperature and the room temperature.
- For the evaluation of the heating system, the collector was installed on the ceiling of a room (2.6 m^2 x 2.15 m) facing north and inclined 20° with respect to the horizontal, the hot air extracted by the air pump is conducted to the interior of the room through pipes previously thermally insulated. The temperature variation of the air entering the room was recorded for the optimum heating speed according to the previous result. This record was made in the process of charging the collector when it is exposed to solar radiation for 2 h and then in the process of discharging the PCM storage system when the incidence of solar radiation ceases or is interrupted.

2.2 Instruments used in the experimentation

Radiometer: UNI-100 mV 1000 W/m^2, with minimum reading of 10 W/m^2, temperature data logger EBRO EBI 40 with sensitivity of 0.1 °C with type K thermocouples, Fluke 179 multimeter, voltage sensitivity: 0.01 V and current intensity: 0.001 A.

Fig. 1 shows a detailed schematic of the developed solar heating system, which incorporates a phase change material (PCM). The system is built around a flat-plate solar air collector-accumulator, integrating solar collection and thermal storage into a single unit. The main components illustrated in the diagram are as follows:(a) Support Structure and Insulation: The main housing of the system is shown, including its overall dimensions and the integrated thermal insulation layer. (b) Thermal Storage System: This section details the configuration of the encapsulated PCM (paraffin) units. The individual dimensions of the units and their spatial arrangement on the absorber plate are specified, highlighting the optimized design for maximizing the heat exchange surface area with the air. (c) System Integration and Installation: The compact, monolithic integration of the collector and accumulator is depicted. This part also indicates the recommended orientation and installation setup for the system within a dwelling.

2.3 Operating conditions for the proposed solar heating system

2.3.1 Climatic conditions for operation of the proposed solar heating system

The case study was carried out in the city of Ayacucho, Peru, located at 2761 meters above sea level, the climate is mild and dry. It is located at a south latitude 13°09'26" and west longitude 74°13'22", its average monthly maximum temperature is 27 °C and the minimum 14 °C. The average annual temperature is 16.1°C and the lowest temperatures below 10 °C are found in the winter months between 22 h and 7 h. The average annual relative humidity is 56 %.

According to the movement of the Sun for the city of Ayacucho, Peru, during the winter months the Sun is declined to the north, months in which there is a higher percentage of sunshine hours, so, a solar technological system takes advantage of the solar energy orienting it to the north with an inclination corresponding to the local latitude. The global average radiation of Ayacucho, Peru is 6.7 KW/m^2, with an average annual solar brightness of 67 %, resulting in an important solar potential to diversify energy for home heating.

Table 1
Collector Dimensions

Feature	Unit	Value
Width	m	0.52
Height	m	0.12
Cross-sectional area	m^2	0.06
Wetted perimeter	m	2.36
Length	m	0.96
Collection area	m^2	0.50

2.3.2 Determination of thermal comfort

The temperature for thermal comfort depends on thermal factors such as air temperature, radiant temperature, air humidity, and air velocity, as well as factors related to the person's clothing, activity, and metabolism. To determine the optimal thermal comfort temperature at which the person expresses thermal satisfaction with the room, we use the expression of Auliciems (Kukukaite 2017):

$$\boldsymbol{To = 17.6 + 0.31Tm} \quad (1)$$

Where: To, Optimal comfort temperature; Tm, Average annual or monthly temperature. For the case of Ayacucho, Peru, the optimal annual average thermal comfort temperature To = 22.59 °C, for the months of May to July (which corresponds to the evaluation stage), the monthly average temperature is 14.9 °C so the optimal comfort temperature is 22.21 °C.

2.4 Solar Collector Dimensioning

The experimental prototype is a flat solar collector with a single air passage, which incorporates on its collector plate the paraffin storage system that operates as a thermal radiator.

2.4.1 Dimensioning of the geometrical characteristics of the prototype of the flat plate solar air collector.

Collector dimensions. The geometrical parameters of the collector affect its thermal performance and influence the air dynamics inside it, and the construction costs (Estrada Piqueras 2018). Given its modular character, 0.5 m^2 was taken as the effective area of the module to evaluate its thermal effect on a test environment of 2.6 m^2. Table 1 shows the dimensions of the collector.

2.4.2 Dimensioning of the thermal and optical characteristics of the materials used to build the solar collector.

Main components of the flat plate solar collector:

- Transparent cover: 1.2 mm thick commercial semi-double glazing was used, with a direct solar radiation transmittance of 0.8.
- Collector or absorber plate: 1 mm thick galvanized iron was used, covered with matte black commercial paint with emissivity 0.9, absorptivity 0.9 and reflectivity 0.1 (Mealla Sánchez, Luis Enrique; Bonaveri Arangoa 2012).
- Support structure. The casing was adapted to the design of the collector operation, the support structure of the transparent cover and the collector plate. The dimensions of the structure are related to the geometrical parameters determined: 15 cm interior height, 52 cm width and 112 cm length. The rectangular structure was built using 1 cm thick plywood, the structure has 7 circles that determine a cold air inlet area of 35.5 cm^2 and a circle of area 81.1 cm^2 for the hot air outlet.
- The thermal insulation is made of 2 cm thick commercial expanded polystyrene, whose properties are shown in Table 2. The base and lateral sides of the collector were insulated to minimize heat losses by conduction.

The thermal efficiency (η) of the solar air collector establishes the ratio between the useful energy and the overall solar energy received by the collector.

$$\boldsymbol{\eta = \frac{Q_u}{A_c G}} \quad (2)$$

Where Q_u is useful energy, A_c is the collector area, G is the incident solar radiation intensity.

Taking reference of the useful energy obtained by the air given by the Hottel-Whillier Bliss equation (Mealla and Bonaveril, 2012), the efficiency results:

$$\boldsymbol{\eta = F_R(\tau\alpha - U_L\frac{T_e - T_a}{G})} \quad (3)$$

Where F_R is the heat removal factor, G is the incident solar radiation intensity, τ is the transmittance of the glass cover, α is the absorption coefficient of the absorber plate, U_L is the overall heat loss coefficient, T_e is the inlet air temperature and T_a is the room temperature.

The useful energy characterizes the thermal energy that allows heating the heat transferring fluid, which is the air, and is given by the equation:

$$\boldsymbol{Q_u = \dot{m}C_p(T_s - T_e)} \quad (4)$$

Where: $\dot{m}$ is the air mass flow rate, C_p is the specific heat of the air, T_s is the collector air outlet temperature, T_e is the collector air inlet temperature.

2.5 Storage system design

2.5.1 Determination of phase change material (PCM)

The phase change material determined is commercial paraffin, due to its favorable thermal properties for low temperature applications, cost and local availability. The paraffin is a non-toxic organic material, stable and does not show overcooling or corrosion and withstands many charge and discharge cycles, it has a melting point of 53 °C and its latent heat of fusion is 132.5 kJ/kg (Janampa 2021). Its disadvantage is the volume change

Table 2
Thermophysical properties of the solar collector materials

Property	Unit	Transparent cover* (Glass)	Absorber plate (galvanized iron)	Insulation	
				**(expanded polystyrene)	Plywood
Specific heat	J/kg K	830	477.2		
Density	Kg/m^3	2200	7874	10	530
Thermal conductivity	W/mK	1.15	80.2	0.042	0.14

Note: * Source González *et al.* (2016). ** Measured by the authors.

Table 3
Energy stored in the thermal storage system with paraffin as PCM

Unit length	cm	98.0
Unit interior height	cm	4.6
Unit inner thickness	cm	1.0
Paraffin solid mass	g	346.82
Room temperature	°C	20.0
Cumulative energy from heating up to 53 °C	kJ	33.91
Cumulative energy per phase change (53 °C)	kJ	45.92
Accumulated energy in one unit	kJ	79.83
Total energy of the storage system (12 units)	kJ	957.93

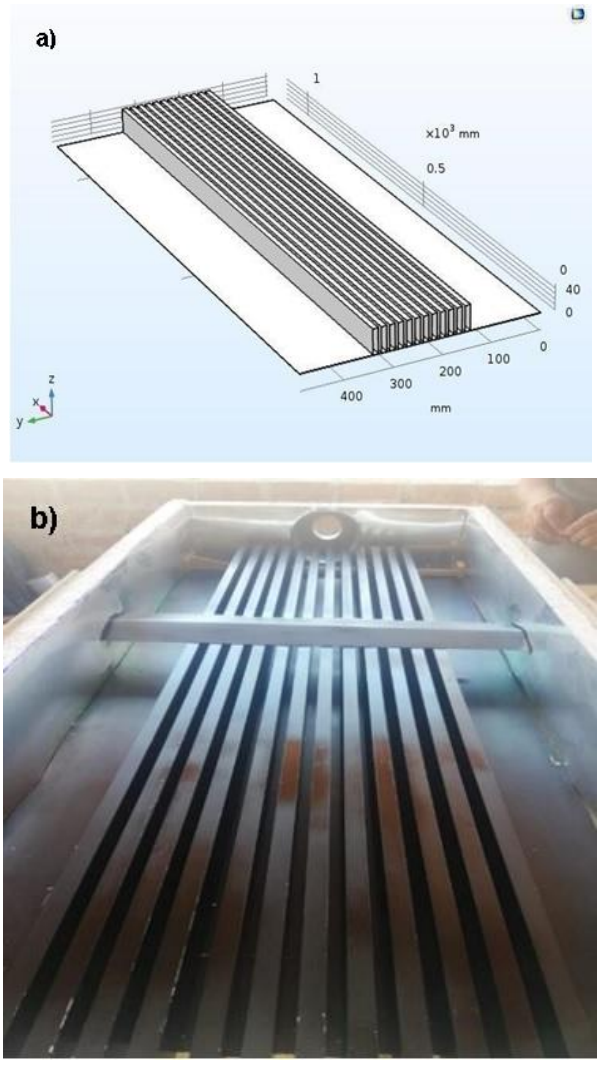

Fig. 2. Thermal storage system composed of 12 units with macroencapsulated PCMs (a) Design (b) Finished and painted matte black and placed on collector plate

from solid to liquid and its low thermal conductivity (Kukukaite 2017).

2.5.2 Storage system with paraffin as PCM

The solar thermal storage unit is based on the macro encapsulation of paraffin in rectangular section aluminum tubes for industrial use, due to its availability and adaptability. The thermal storage unit is 98 cm long and has an interior space of 1 cm x 4.6 cm. Each unit is filled with 346 g of wax, properly sealed between the base and 10 cm away from the upper end, leaving 10 % of free space inside. The top 10 cm are tubular fins to facilitate heat transfer to the air, optimizing its function as a

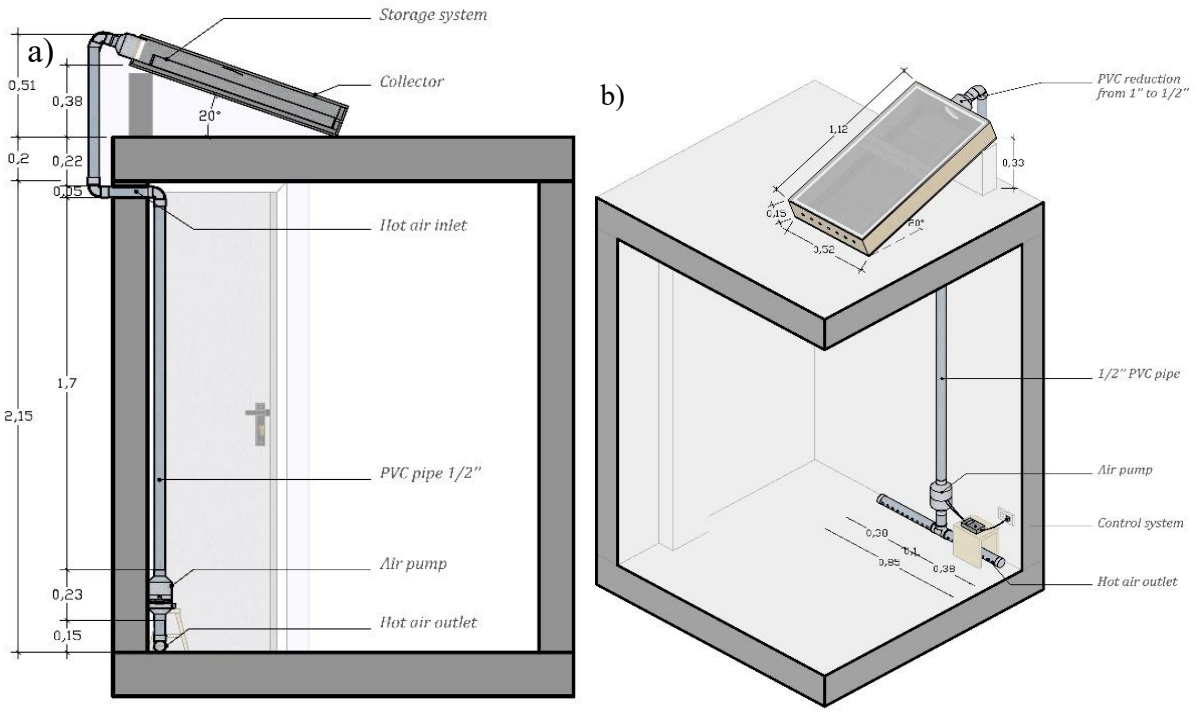

Fig. 3. Heating system installation scheme: solar collector, PCM storage system, duct orpiping systems, air pump, pump extraction speed control system

radiator and directing the heat flow towards the collector outlet. The energy available in each unit is about 79 kJ, accumulated during heating from room temperature to melting temperature and subsequent phase change. The energy stored by the storage system is 958 kJ, as shown in Table 3.

Fig. 2 shows the layout of the 12 solar thermal storage units; each unit consists of an aluminum tube of rectangular section; these tubes were filled with kerosene up to 90 % of their capacity, the remaining 10 % was filled with air at a free atmosphere, and the ends of these tubes were hermetically sealed to avoid losses. The distance between each accumulator unit is 1 cm, to improve heat transfer to the air.

2.6 Forced air flow system design

2.6.1 Hot air flow rate requirement

To maximize the heat transfer from the absorber plate of the collector to the surrounding air, the air flow must be turbulent with a velocity between 1 m/s and 1.4 m/s (Kukukaite 2017), this value limits the fan speed to drive the hot air. The speed at which the room heats up depends on the speed at which the air enters, likewise, the thermal sensation depends on the speed of air movement. The air speed in comfort conditions should be 0.18 m/s to 0.24 m/s in summer and 0.15 m/s to 0.20 m/s in winter (Regulations for Thermal Installations in Buildings (RITE)(Moscoso Cáceres 2016). For a speed of 0.15 m/s for each 0.08 m/s increase, the thermal sensation decreases by 1 °C (Kukukaite 2017).

2.6.2 Forced air flow system components

Air pump. The air pump built has an axial cooler component, powered by 220 V-AC, with a power of 17.6 W, 0.08 A - 60 Hz - 2500 rpm. It was built on two PVC reducer tubes of 4 to 2 inches. The fan of the pump is connected to an electronic controller that regulates the rotation speed and consequently the extraction pressure of the pump, in order to regulate the hot air outlet velocity and keep it within the comfort limits.

Air distributor. The hot air is conducted to the lower part of the interior of the test environment, through a PVC duct of 2 inches in diameter. To homogenize the distribution of hot air and to reduce its speed of entry into the room a horizontal pipe (distributor) was used. It has 20 holes with a total area greater than the area of the 2-inch pipe. This system acts by interrupting the flow and generating turbulence, thus reducing the speed of air entering the room to less than 0.24 m/s.

2.6.3 Heating system installation scheme

Fig. 3 shows the dimensions, components and installation scheme of the heating system on the ceiling of a test room.

The operation of the system begins with the photothermal conversion in the flat solar collector, where the absorber plate has the capacity to absorb solar energy and a low emissivity, so that the transport medium, which is air, is able to take the greatest amount of thermal energy from the absorber plate and the glass cover is able to confine the infrared energy emitted from the plate to the interior. Simultaneously, during the incidence of solar radiation, the storage system absorbs thermal energy so that the phase change material, paraffin, increases its temperature until it changes from solid to liquid state, accumulating energy by temperature change and latent heat. During the charging process of the storage system, the air in the collector is heated by convection and radiation from the plate and the outer surface of the storage system; and when the incidence of solar radiation is interrupted or decreases, the process of discharging the storage systems begins, relaying the thermal energy accumulated to the air by both conduction and radiation. During the charging and discharging process, the radiator of the storage system units optimizes and directs the thermal flow. The hot air generated in the collector is forced to circulate through the 2-inch (5.08 cm) tubes by the air pressure exerted by the pump and the temperature gradient of the solar

collector. Inside the 2.6 m x 2.15 m room, the hot and cold air masses are recombined, and by thermal equilibrium the temperature is increased until the required comfort temperature is reached, the room is closed to prevent external air from entering.

3. Results and discussion

The control of the pump air flow was carried out to determine the optimum position of the extractor and the optimum air extraction speed. The temperature variation of the collector plate and of the hot air entering and leaving the collector was measured, and the data was used to determine thermal parameters of the collector with and without incorporating the storage system with PCM. The collector was installed on the roof of the test environment, the ducts and the air pump inside the test room. By placing the sensors on the collector, and the pump in the room, the variation of the air temperature of the test environment was determined during the charging and discharging process of the collector-accumulator.

3.1 Results of hot air flow control to the test environment

The control was done by measuring the temperature of the hot air reaching the test environment extracted by the pump for different flow rates. The air pump is equipped with an electronic controller that allows the fan speed to be varied by means of a selector. To take data on the temperature of the air entering the

Table 4.
Increase in the temperature of the air entering the ambient test environment for different velocities

Parameters	**Pump at the end of the pipeline**				**Pump in the middle of thepipeline**			
	m	I_1	I_2	M	m	I_1	I_2	M
V (±0.01 m/s)	1.26	2.47	2.85	2.92	0.52	1.09	1.24	1.24
ΔT (±0.1 °C)	0.7	4.4	2.9	1.3	1.7	3.7	2.2	1.0
ΔT/t (°C/min)	0.1	0.4	0.3	0.1	0.2	0.4	0.2	0.1

Note: Four pump selector positions were considered: corresponding to the minimum speed (m), maximum speed (M) and two intermediate positions (I_1 and I_2) between minimum and maximum.

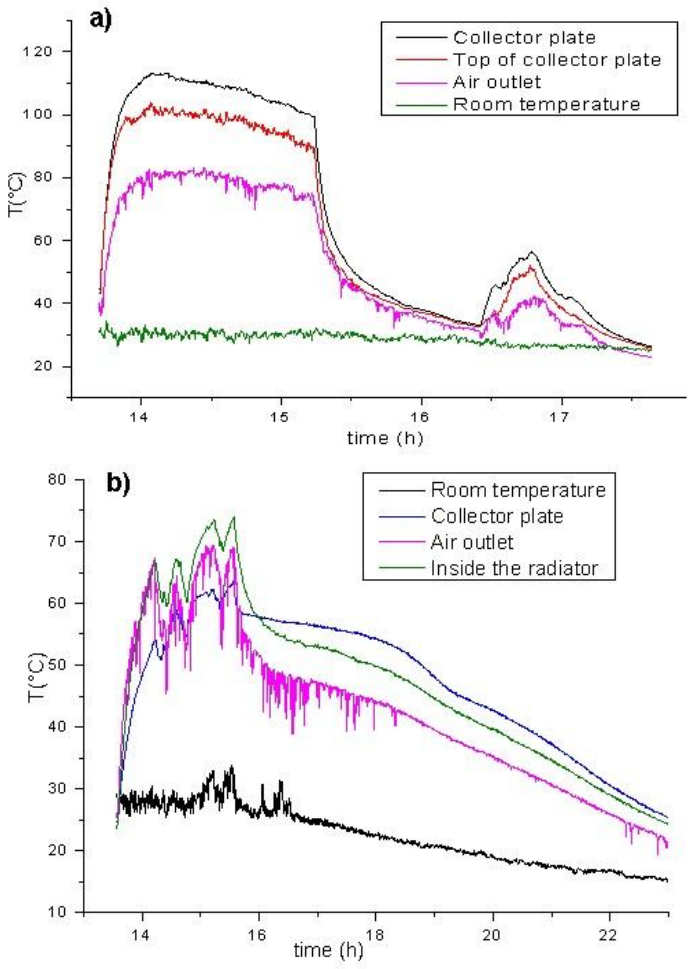

Fig. 4: Temperature variation in the flat plate solar collector (a) without storage system for an average radiation intensity of 774 W/m^2 at charging (b) with storage system for an average radiation intensity of 810 W/m^2 at charging

room, the controller selector was set to four positions: one corresponding to the minimum speed (m), one to the maximum speed (M) and two intermediate positions (I1 and I2) between the minimum and maximum. The pump was placed in two positions to analyze its best performance with respect to the floor: one in an intermediate position 80 cm away from the room surface and another at the duct outlet end, 10 cm away from the room surface. Table 4 shows the results of the temperature variation per minute of the hot air entering the room for different extraction velocities at the two pump locations.

From Table 4, for the intermediate positions (I1 and I2) of the electronic controller selector, a higher test environment air temperature increase is found, from 2.2 °C to 4.4 °C for an air extraction flow rate of 2.47 m/s to 2.85 m/s and 1.09 m/s to 1.24 m/s, respectively for the positions at 10 cm and 80 cm from the extractor. So, the optimum extractor position was taken as 10 cm from the ground and with a flow rate of 2.47 m/s at the pump.

3.2 Thermal performance of the flat plate solar collector

The heating capacity of the collector was evaluated during 2 h of solar radiation incidence and the cooling capacity, when the radiation is interrupted. With the data obtained, the instantaneous efficiency of the solar collector with and without PCM was determined. The data shown below are experimental results.

3.2.1 Results of the flat plate collector

For the case in which the collector does not use the PCM, it is charged from 13:30 h to 15:20 h and uncharged from 13:20 h to 17:30 h (Fig. 4-a), and for the collector with PCM it is charged from 13:30 h to 15:30 h and uncharged until 23:00 h (8 h) (Fig. 4-b); during these tests the air pump is not used. Fig.6 4-a, shows the stagnation temperature of the collector which is in the order of 110 °C for an average solar radiation of 774 W/m^2. The stagnation temperature is the maximum temperature of the plate when the collector reaches thermal equilibrium with the outside; under these conditions, the maximum temperature of the air at the collector outlet was 80 °C. Likewise, the temperature of the plate and the air increases rapidly at a rate of 3.4 °C/min and when the incidence of solar radiation on the collector is interrupted, the rapid drop in the temperature of the plate is noticeable. In the first 3 minutes it decreased from 100 °C to 60 °C, at a rate of 13 °C/min, due to the loss of thermal energy to the outside due to the high temperature gradient with respect to the outside.

When the collector uses the storage system with PCM (Fig. 4-b), the collector plate reached a maximum temperature of 75

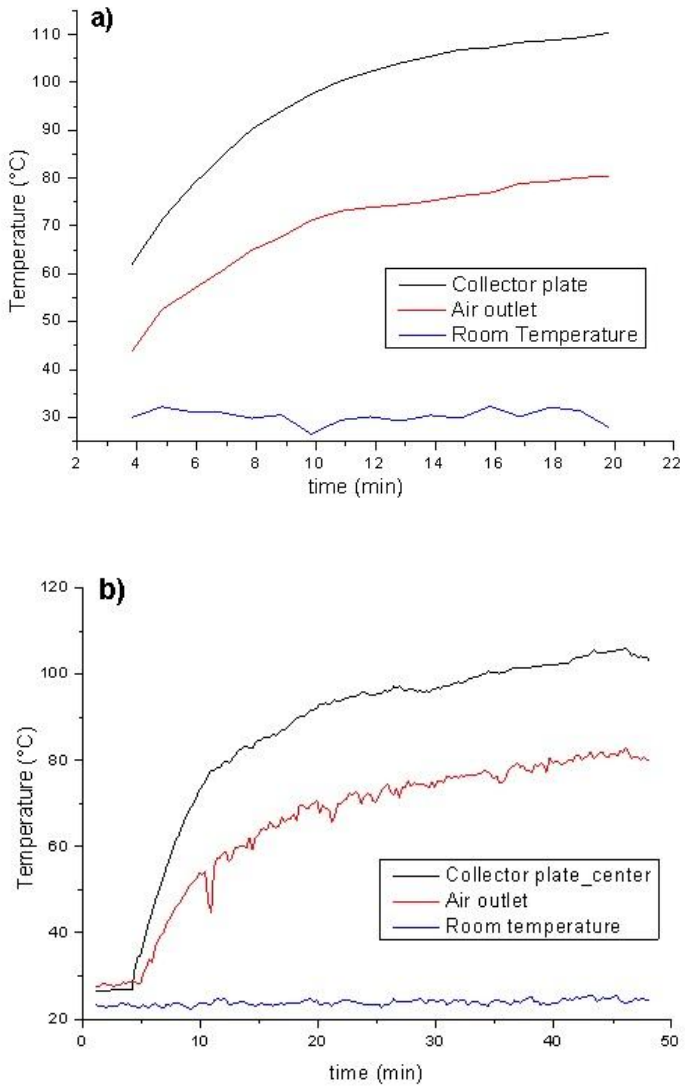

Fig. 5: Stagnation temperature in the flat plate collector for an average radiation intensity of (a) 774 W/m^2 and (b) 813 W/m^2

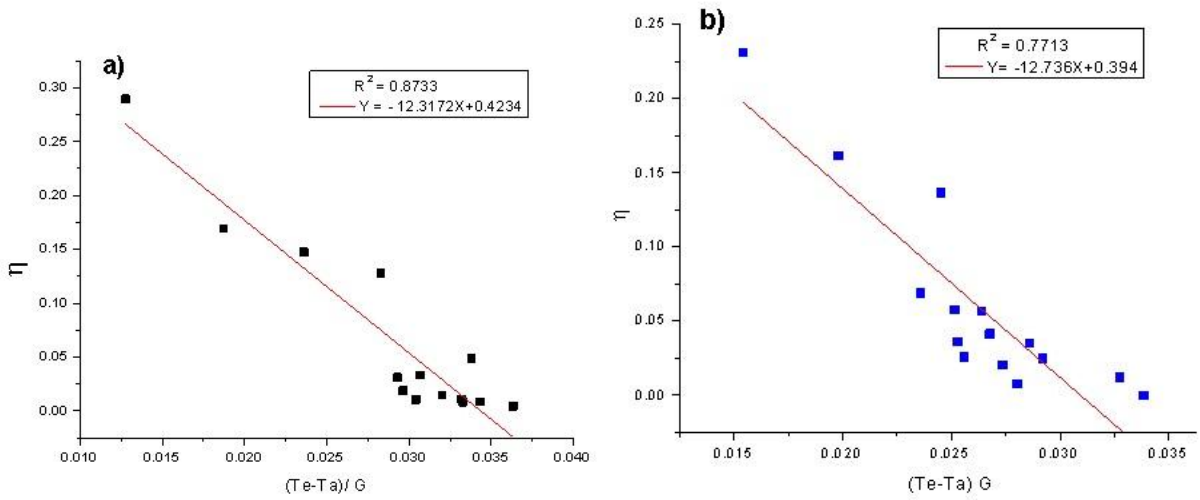

Fig. 6. Instantaneous efficiency of the flat plate solar collector for an average radiationintensity of (a) 774 W/m^2 and (b) 813 W/m^2

°C and the air temperature at the collector outlet 60 °C, for an average radiation incidence of 810 W/m^2 in the 2 h of charge. When the incidence of solar radiation was interrupted, the temperature of the plate and the outgoing air decreased slowly at a rate of 0.10 °C/min and 0.11 °C/min respectively. This shows the effect of the phase change material that stabilizes the temperature between 40 °C and 50 °C for a period of 2.5 h and maintains a temperature higher than the ambient temperature by more than 10 °C for up to 4.5 h more. Fig. 4-b shows the variation of the air temperature inside the radiator in a storage system unit reaching a maximum value of 74 °C being higher than that of the collector plate. The result reveals the function of the radiator, that during the charging process its temperature is higher than that of the collector plate and during the discharge it decreases as a consequence of the heat transfer to the circulating air.

Fig. 5 shows the collector stagnation temperature of 110 °C and 105 °C for an average radiation of 774 W/m^2 and 813 W/m^2 respectively which during the test minutes tends to be uniform. To determine the thermal parameters of the collector, from the data in Fig. 5, the thermal efficiency was found using equation (2) and relating it to equation (3), the heat removal factor and the overall loss coefficient of the collector were determined.

The useful heat was determined for 2-minute intervals using equation (4) for 50 minutes where a constant value of solar radiation incidence is recorded around midday. For the efficiency graph (Fig. 6 and Fig. 8), the average value between the fluid outlet temperature and the ambient temperature was considered as the inlet temperature in equation (3), since the temperature at which the air enters the collector is the room temperature. Fig. 6 shows the instantaneous efficiency of the collector without incorporating the PCM storage system for radiations of 774 W/m^2 and 813 W/m^2, respectively; the mass flux for natural flow in the collector was determined to be in the order of 8 g/s to 9 g/s.

From the collector instantaneous performance equation according to Fig. 6 and equation (3), the removal factor and the overall collector loss coefficient are obtained as shown in Table 5.

3.2.2 Results of the flat collector with PCM thermal storage system and forced flow

To determine the thermal behavior of the collector incorporating the thermal storage system with paraffin, the collector was oriented towards the north and the incidence of the sun's rays was allowed for an interval of 2 h (from 12:00 h to

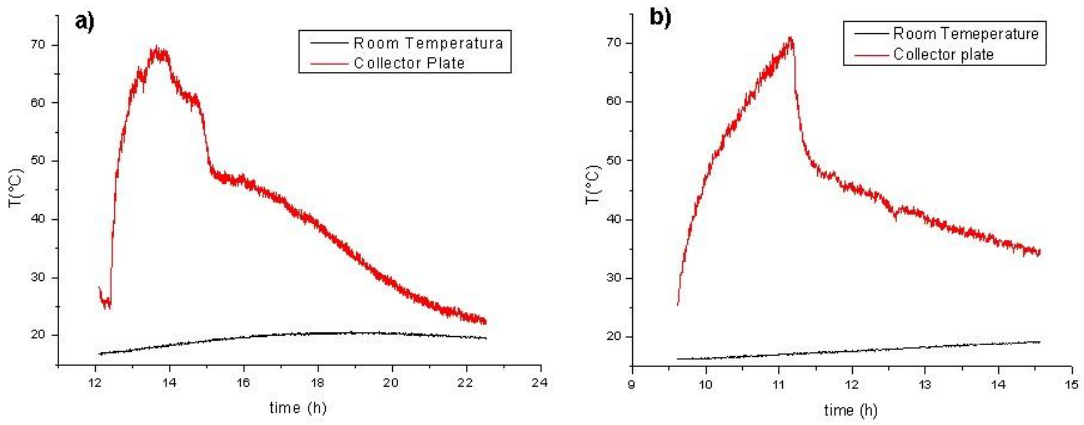

Fig. 7: Air temperature variation of the flat plate solar collector with storage system and forced flow. Radiation (a) 854 W/m^2 (b) 785 W/m^2, in the 2 h of charge

Table 5.
Overall loss coefficient and removal factor of the flat plate solar collector with and without PCM

Solar collector	Solar radiation intensity: G (W/m^2)	($\tau\alpha$)	Mass flow (g/s)	Overall loss coefficient:U_L ($W/m^{2o}C$)	Heat removal factor (FR)	Optical efficiency(%)
Without PCM Storage system	744	0.72	8.5±0.5	20.9±7.6	0.59±0.20	42.3
	813	0.72	9.2±0.5	23.7±6.6	0.55±0.15	39.4
With PCM storage system	785	0.72	22.4±0.5	20.9±5.0	0.76±0.18	54.8
	854	0.72	22.4±0.5	26.8±9.5	0.76±0.22	54.8

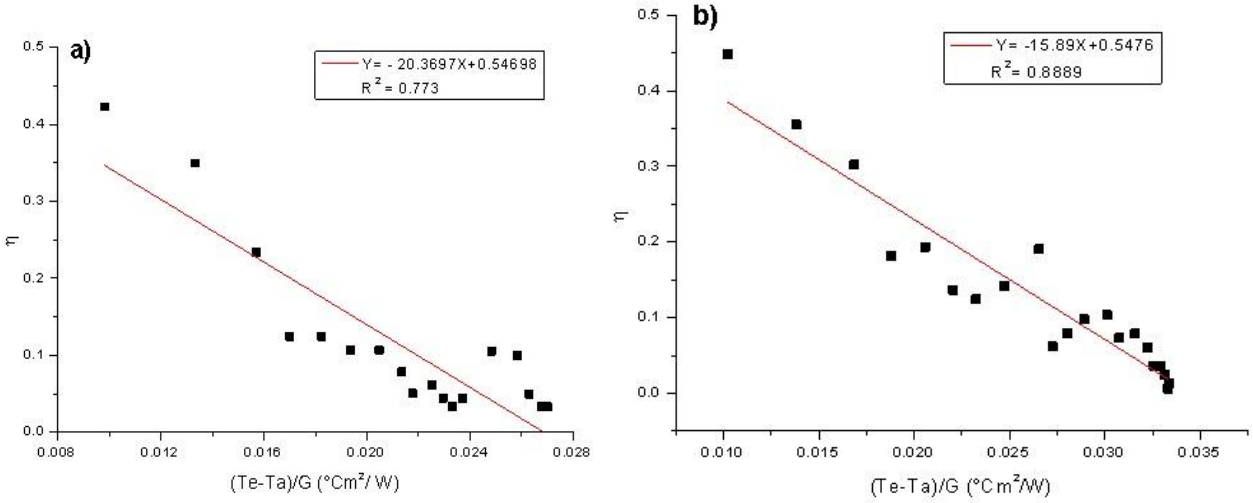

Fig. 8: Instantaneous efficiency of the flat plate solar collector with PCM storage system (a) for 854 W/m^2 and (b) for 785 W/m^2

14:00 h), where the storage system is charged with thermal energy; then, the incidence of solar radiation was interrupted and the storage system began to discharge (14:00 h to 22:00 h), see Fig. 7.

Fig. 7 shows that the maximum air temperature at the collector outlet was 70 °C for an average radiation incidence of 854 W/m^2 in the 2 h of charge. When the solar radiation incidence was interrupted, the outgoing air temperature decreased rapidly for one hour (14:00 h to 15:00 h) and in the following 7 h it decreased more slowly at a rate of 5 °C/h; this shows the effect of the phase change material stabilizing the temperature. From the data in Fig. 7, the instantaneous efficiency curve of the flat plate solar collector with PCM is obtained, which is shown in Fig. 8-a for 854 W/m^2 and is additionally obtained for 785 W/m^2 (Fig. 8-b).

Fig. 8 shows the instantaneous efficiency of the collector, for an average radiation intensity of 854 W/m^2 and 785 W/m^2 respectively, and comparing to the efficiency equation (3) we obtain the characteristic thermal parameters of the flat solar air collector when incorporating the paraffin storage system, these parameters are shown in Table 5.

Table 5 shows that the maximum instantaneous efficiency of the collector improves substantially when the thermal storage system with paraffin is incorporated, being of the order of 54.7 % in relation to 41 % when PCM is not used, since the heat removal factor improves from 0.57 to 0.76 by increasing the contact area of the heat transfer fluid and also by increasing the mass flow from 9 g/s to 22 g/s, given that as the air flow rate increases, the efficiency of heat transfer to the air increases.

Regarding the overall loss coefficient, a high value of 22 W/m^2 °C was found, which means a loss of 22 W per square meter of surface and per degree Celsius, which is related to the low-cost design where the thermal properties of the materials used in the collector are not the most efficient, materials such as a thin glass transparent cover, expanded polystyrene and wood as insulation of the base and the lateral side of the collector.

3.3 Heating of the test environment

We disclose the results of the test of heating the air inside the room, for this purpose we record the temperature of the air at the outlet of the collector, the temperature in the center inside the distributor, and the air temperature 20 cm and 40 cm away from the room surface.

3.3.1 Results of the variation of the temperature of the air entering the room.

For the evaluation of the temperature increase of the air that entered the room, the pump is located at the bottom of the duct, 10 cm away from the surface of the test environment and the electronic controller extracted air with a velocity of 2.5 m/s, The air flow distributor tube is placed at the outlet of the

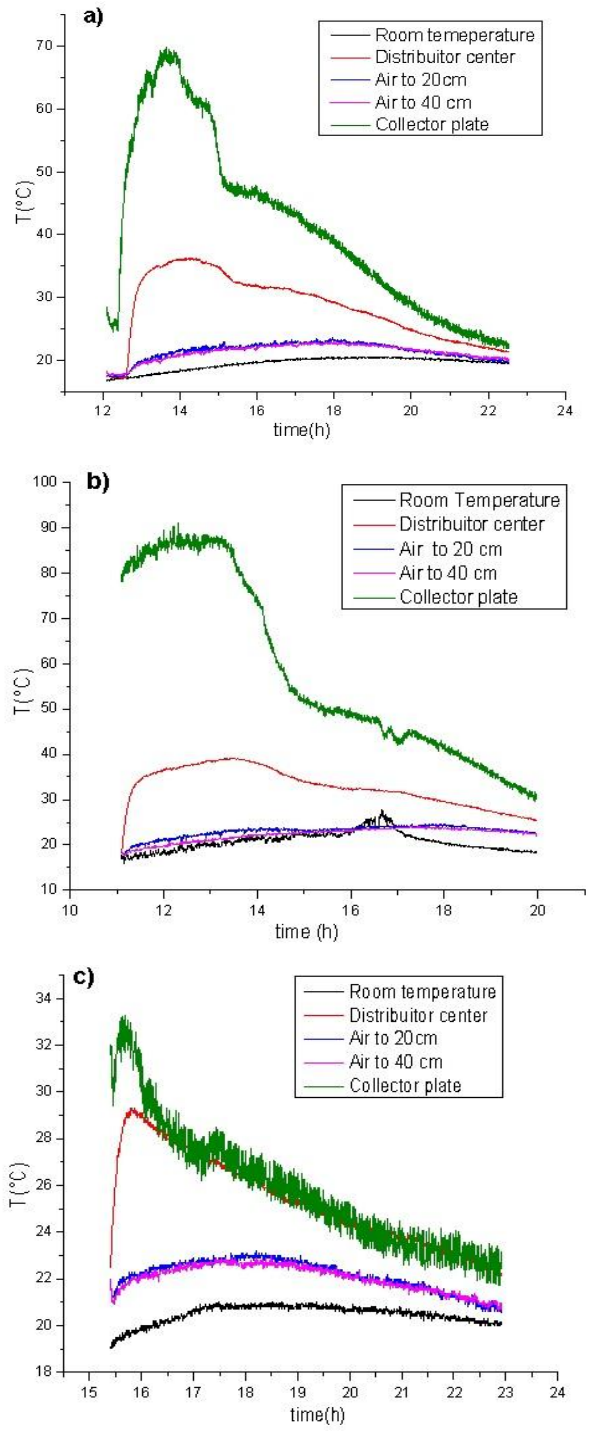

Fig. 9: Temperature variation inside the room for a solar radiation intensity of (a) 935 W/m^2 854 W/m^2 and (c) 698 W/m^2 during the storage system charging process

extractor. Fig. 9, shows the variation of the air temperature at the outlet of the collector, the temperature of the test room at 20 cm and 40 cm from the floor, the room temperature and the temperature at the center of the distributor.

Fig. 9-a, corresponds to an average solar radiation incidence of 935 W/m^2, during two hours of collector-accumulator system charging, from 11:10 h to 13:10 h. Then the sun incidence was interrupted to evaluate the thermal influence of only the storage system until 20:00 h. The results shown indicate that the temperature of the air leaving the pump exhaust fan is in the order of 34 °C to 39 °C during the charging stage of the collector, generating a temperature of the air inside the environment, at 20 cm and 40 cm above the surface of the room, in the order of 22 °C and 20.7 °C respectively (Fig. 9-a), with an average room temperature for that interval of 18.5 °C. For the discharge stage of the storage system, starting at 13:30, the temperature of the extracted air reduces from 39 °C to 25 °C in 7 h (Fig. 9-a), but the temperature of the room air at 20 cm and 40 cm above the ground remains approximately constant at 23

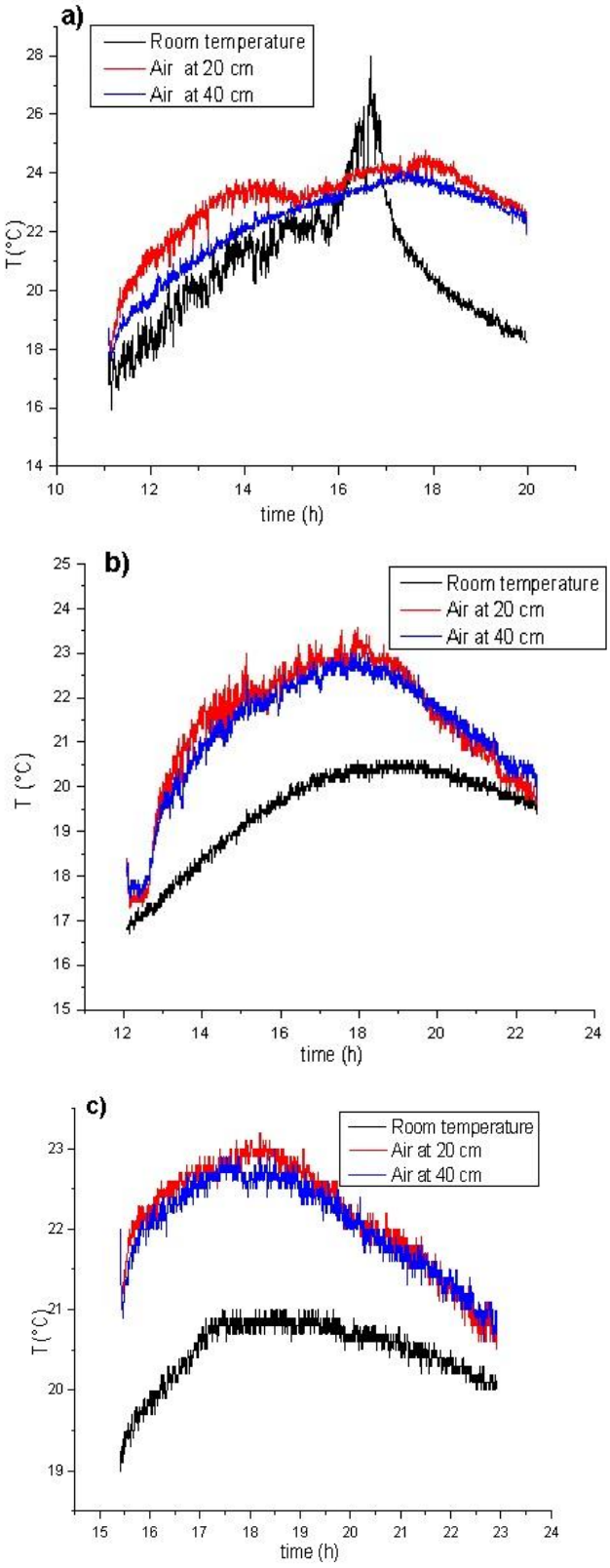

Fig. 10: Air temperature of the room at 20 cm and 40 cm from the floor surface, for (a) 935 W/m^2 (b) 854 W/m^2 (c) 698 W/m^2

Table 6.
Average temperature of the air entering the test environment, for an interval of 2 h ofcollector-accumulator charging

	Radiation during charging	Comfort temperature*	Room temperature (Max-Min)		Discharge time	Air temperature**			
						Charging(°C) (±0.1 °C)		Discharging (°C) (±0.1 °C)	
Date	G(W/m²) (±10 W/m²)	(°C) (±0.1 °C)	(°C) (±0.1 °C)		(h)	20 cm	40 cm	20 cm	40cm
15/07/23	935	22.2	28.0	15.9	7	22.0	20.7	23.6	23.0
17/07/23	854	22.2	20.6	16.7	7	21.0	20.5	22.2	22.0
18/07/23	698	22.2	21.0	19.0	5	22.3	22.1	22.1	22.0

* Outdoor ambient temperature of the test dwelling during the thermal accumulator's charge-discharge cycles, showing maximum and minimum values.
** Indoor air temperature of the test dwelling

°C (Fig. 10-a and Table 6) for 7 h, close to the estimated thermal comfort temperature of 22.2 °C and 4 °C higher than the outdoor temperature of 18 °C; thus revealing that the paraffin PCM of the solar thermal storage tank fulfills its function of stabilizing the temperature of the air inside the room.

Fig. 10-a, 10-b and 10-c, show the indoor air temperature of the test environment for radiations of 854 W/m², 698 W/m² and 698 W/m² respectively, whose characteristic values are shown in Table 6. Table 6 shows the results obtained for the air temperature of the test room, of area 2.6 m² and 2.15 m in height, measured at 20 cm and 40 cm above the floor, both at the collector charging stage when it is exposed to the sun, and in the discharge stage of the storage system when the incidence of solar radiation on the collector is interrupted. For the incidence of solar radiation on the collector of 854 W/m², the air temperature reaches 21 °C to 20.5 °C for 20 cm and 40 cm above the ground, respectively and during discharge the temperature is maintained around 22 °C for 7 h, when the average temperature of the outdoor environment is 18.6 °C. For 698 W/m², there is a difference of 1.3 °C to 1.6 °C during the charging process and no significant difference is shown during discharge; the differences shown were due to the influence of other external factors such as the outside air velocity, which affects the heating capacity of the collector, the intermittency of solar radiation, etc. These values show that the thermal comfort estimated for the test period of the environment used with a collector module of 0.53 m² is guaranteed mainly at night hours where the air temperature inside the room remains constant at 22 °C for up to 7 h, higher than the temperature of the outside environment by 3 °C to 4 °C.

3.4 Discussion

The heating system proposed in this work has as solar energy collector a flat plate solar collector that uses air in a single pass as heat transferring fluid, unlike flat plate collectors with double air pass (Sudhakar and Cheralathan 2021) and heating systems with vacuum tube collectors known for their greater efficiency and more expensive than those proposed in this work (Shabgard, Song, and Zhu 2018) (Luo *et al.* 2017).

The collector-accumulator designed in this work is characterized by the fact that the collector and storage system constitute a unit, the radiator-type storage system is incorporated into the collector on the flat metal plate. This proposal resembles the model that encapsulates paraffin in small spherical balls mounted in the holes of the absorber plate to increase the radiation area (Sudhakar and Cheralathan 2021). Most of the literature reviewed shows solar heating systems where the collector and the storage tank are separate components (Z. Wang *et al.* 2019) (Z. Wang *et al.* 2020), and operate independently. The radiator-type storage system contains macroencapsulated paraffin in rectangular aluminum tubes with tubular fins at the upper end that optimized its radiator function by increasing the contact area with the air as heat transferring fluid, which is evident in Fig. 4-b, where the air temperature reaches values of the order of 74 °C for 810 W/m² during the collector charging process, which shows that it will improve the transfer of thermal energy, and that during the discharging process it directs the thermal flux towards the collector's air outlet.

The heating system proposed in this research, was approached as a modular, simple, replicable design, used low-cost materials; given, as it is argued, that the most promising collector should achieve the best thermal efficiency, ease of fabrication and low cost (Ammar *et al.* 2020). The proposed system can be coupled for higher energy requirements; it contains 4 kg of paraffin distributed in 12 rectangular storage units measuring 98 cm, spaced 1 cm between each unit; unlike the one investigated by Z. Wang *et al.* (Z. Wang *et al.* 2018), who developed a storage system based on microtube arrays where they used 21 kg industrial paraffin wax. The flat plate air collector designed in our proposal, presents an optimum efficiency or maximum instantaneous efficiency of 41 % (Table 5) operating in free flow without PCM storage system and for a mass flow 9 g/s, the hot air leaving the collector reaches temperatures in the order of 80 °C for a solar radiation of 774 W/m² (Fig. 5). This result fits with the 39 % efficiency result presented by M. Hanif et al. (Hanif *et al.* 2018) for free-flowing collectors with a mass flow rate of 0.5 kg/s. In turn, Martinez and Arguello (Martínez Gómez and Argüello Bravo 2020) obtain a collector efficiency of 59.01 % with hot air outlet temperature of 94 °C. The result presented by Estrada (Estrada Piqueras 2018) on a forced collector, single-pass, is of 51.88 % of average efficiency with a mass flow of 0.0348 kg/s for 1 m² of the collector and an average solar radiation of 820 W/m². Wang *et al.* (D. Wang *et al.* 2019) obtained a collector efficiency of 61.5 % and an air outlet temperature of 42.1 °C (Z. Wang *et al.* 2019). In our proposal, incorporating the accumulator with PCM in forced flow and inclined 20° with respect to the horizon increases the maximum collector efficiency up to 54.8 % (Table 5) as a consequence of the increase of the removal factor to 0.76 for a mass flow of 23.6 g/s. In this sense, Sudhakar & Cheralathan (Sudhakar and Cheralathan 2021) investigated the thermal performance of a double pass collector with and without PCM, and obtained an average efficiency of the conventional absorber plate without PCM of 31 %, for the absorber plate with PCM of 39 %, and for the inclined absorber plate with PCM of 43 %.

According to Table 6, the heating temperature of the air inside the environment produced by the heating system designed in this work, was equal to 20 °C – 22 °C, during the charging process of the collector-accumulator when the system has captured the solar radiation energy during a two-hour interval. In the discharge stage of the collector-accumulator, the air temperature was maintained between 22 °C to 23 °C for an interval of more than 6 h, thus revealing that the air temperature of the test environment remains constant even though the outdoor environment temperature changes by increasing or decreasing (Table 6 and Fig. 10). The results obtained show that the test environment temperature is 2 °C to 3 °C higher than the outdoor temperature of 19 °C to 20 °C during the daytime, and at night it is 3 °C to 4 °C higher than the outdoor temperature, which drops down to 16 °C to 18 °C (Fig. 10). Nonetheless, thermal comfort is not only a factor related to air temperature, but also to other weather conditions such as wind speed and air humidity, solar radiation and duration of direct sunshine (Maka and Alabid 2022). In our work, the air flow inlet velocity to the test environment has been controlled by the air flow control system and the air distributor which reduced the air velocity in the order of 0.2 m/s. The results of the indoor air heating temperature of the test environment with the heating system proposed in this work turned out to be within the range obtained for a light house, where an increase of the average indoor air temperature by 3.8 °C during the daytime is reported (Kou *et al.* 2022). An increase of the minimum indoor operating temperature between 5.1 °C and 10.5 °C by optimizing the thermal properties of the exterior and interior envelopes of the house was also attained, improving the indoor thermal sensation between 36 % and 100 % (Kou *et al.* 2023). These results differ from our work since we only focused on the thermal control of the system and did not optimize the thermal properties of the envelopes of the test environment, a control that would improve maintaining the comfort temperature and the efficiency of the system for longer.

4. Conclusions

This research presents the design, construction, and thermal evaluation of an integrated solar heating system in which the collector and thermal storage unit form a single modular block. The key innovation lies in the radiator-type thermal storage unit, which uses paraffin as a phase change material (PCM) encapsulated in twelve finned aluminum tubes. This design functions not only as an energy storage medium but also as a passive radiator, optimizing heat distribution and ensuring uniform heat release during both day and night.

Experimental results validate the system's thermal performance: the outlet air temperature from the collector exceeded 70 °C, and thermal comfort conditions were maintained inside the test room (20.5 °C –23.6 °C), with a temperature difference of up to 4 °C compared to the outdoor environment for extended periods. The use of PCM stabilized the indoor temperature by storing and releasing latent heat during discharge cycles.

These findings confirm that the proposed prototype represents a technological innovation in modular passive solar system design. It integrates heat collection, storage, and radiation into a single, low-cost, and highly reproducible device. Its constructive simplicity and thermal efficiency make it a viable alternative for implementation in cold climates, where the demand for sustainable heating is critical. This work opens new perspectives for developing sustainable residential heating solutions in rural and hard-to-reach areas.

Acknowledgments

Author Contributions: K.J.: Conceptualization, methodology, formal analysis, writing—original draft, H.C.; supervision, resources, project administration, O.M.; writing—review and editing, project administration, validation, O.C.; writing—review and editing, project administration, validation, J.O.; writing—review and editing, validation. All authors have read and agreed to the published version of the manuscript.

Funding: The author(s) received no financial support for the research, authorship, and/or publication of this article.

Conflicts of Interest: The authors declare no conflict of interest.

References

Akbari, V., Naghashzadegan, M., Kouhikamali, R., Afsharpanah, F., & Yaïci, W. (2022). Multi-Objective Optimization of a Small Horizontal-Axis Wind Turbine Blade for Generating the Maximum Startup Torque at Low Wind Speeds. *Machines,* 10(9). https://doi.org/10.3390/machines10090785

Algarni, S. (2023). Evaluation of Performance Optimization of a Hybrid Solar Flat Plate Collector Integrated with Phase Change Material and Water Heat Sink. *SSRN Electronic Journal.* https://doi.org/10.2139/ssrn.4326076

Ammar, M., Mokni, A., Mhiri, H., & Bournot, P. (2020). Numerical analysis of solar air collector provided with rows of rectangular fins. *Energy Reports,* 6, 3412–3424. https://doi.org/10.1016/J.EGYR.2020.11.252

Athienitis, A. K. (2007). Design of a Solar Home with BIPV-Thermal System and Ground Source Heat Pump. 2nd Canadian Solar Buildings Conference Calgary, June 10 – 14, 2007, 1–9.

Bać, A., Nemś, M., Nemś, A., & Kasperski, J. (2019). Sustainable integration of a solar heating system into a single-family house in the climate of Central Europe-A case study. *Sustainability* (Switzerland), 11(15). https://doi.org/10.3390/su11154167

Badiei, Z., Eslami, M., & Jafarpur, K. (2020). Performance improvements in solar flat plate collectors by integrating with phase change materials and fins: A CFD modeling. *Energy,* 192. https://doi.org/10.1016/j.energy.2019.116719

Chi, F., Wang, R., & Wang, Y. (2021). Integration of passive double-heating and double-cooling system into residential buildings (China) for energy saving. Solar Energy, 225, 1026–1047. https://doi.org/10.1016/j.solener.2021.08.020

Estrada Piqueras, A. (2018). Diseño, construcciòn y ensayo de un colector solar de aire. Universidad Politècnica de Madrid. https://blogs.upm.es/sostenibilidadupm/wp-content/uploads/sites/759/2020/03/TFM-Alberto-Estrada.pdf

Godoy-Vaca, L., Vallejo-Coral, E. C., Martínez-Gómez, J., Orozco, M., & Villacreses, G. (2021). Predicted medium vote thermal comfort analysis applying energy simulations with phase change materials for very hot-humid climates in social housing in ecuador. *Sustainability (Switzerland),* 13(3), 1–31. https://doi.org/10.3390/su13031257

Golovchak, R., Plummer, J., Kovalskiy, A., Holovchak, Y., Ignatova, T., Trofe, A., Mahlovanyi, B., Cebulski, J., Krzeminski, P., Shpotyuk, Y., Boussard-Pledel, C., & Bureau, B. (2023). Phase-change materials based on amorphous equichalcogenides. *Scientific Reports,* 13(1). https://doi.org/10.1038/s41598-023-30160-7

González Bayón, J. J., Borrajo Pérez, R., & Koulibaly, A. (2016). Thermal Performance of flat solar collectors for air heating working in natural convection. A parametric analysis. *Ingeniería Mecánica*, 19(1), 68–77. https://www.redalyc.org/pdf/2251/225146302001.pdf

Gosztonyi, S., Stefanowicz, M., Bernardo, R., & Blomsterberg, Å. (2017). Multi-active façade for Swedish multi-family homes renovation - Evaluating the potentials of passive design measures. *Journal of Facade Design and Engineering,* 5(1), 7–21. https://doi.org/10.7480/jfde.2017.1.1425

Hanif, M., Khan Khattak, M., Khan, M., Ramzan, M., & Abdurab. (2018). Energy, exergy and efficiency analysis of a flat plate solar collector used as air heater. *Sains Malaysiana,* 47(5). https://doi.org/10.17576/jsm-2018-4705-24

Izadi, M., Taghavi, S. F., Neshat Safavi, S. H., Afsharpanah, F., & Yaïci, W. (2023). Thermal management of shelter building walls by PCM macro-encapsulation in commercial hollow bricks. *Case Studies in Thermal Engineering,* 47. https://doi.org/10.1016/j.csite.2023.103081

Janampa, K. (2021). Acumulador solar térmico de placa compacta con material de cambio de fase para secadores familiares. *Tecnia*, 31(1), 56–66. https://doi.org/10.21754/tecnia.v21i1.1097

Koca, A., Oztop, H. F., Koyun, T., & Varol, Y. (2008). Energy and exergy analysis of a latent heat storage system with phase change material for a solar collector. *Renewable Energy*, 33(4), 567–574. https://doi.org/10.1016/j.renene.2007.03.012

Kong, X., Wang, L., Li, H., Yuan, G., & Yao, C. (2020). Experimental study on a novel hybrid system of active composite PCM wall and solar thermal system for clean heating supply in winter. *Solar Energy*, 195. https://doi.org/10.1016/j.solener.2019.11.081

Kou, F., Gong, Q., Zou, Y., Mo, J., & Wang, X. (2023). Solar application potential and thermal property optimization of a novel zero-carbon heating building. *Energy and Buildings*, 279. https://doi.org/10.1016/j.enbuild.2022.112688

Kou, F., Shi, S., Zhu, N., Song, Y., Zou, Y., Mo, J., & Wang, X. (2022). Improving the indoor thermal environment in lightweight buildings in winter by passive solar heating: An experimental study. *Indoor and Built Environment,* 31(9), 2257–2273. https://doi.org/10.1177/1420326X221091448

Kukukaite, D. (2017). Sistema automática de control térmico para viviendas unifamiliares aprovechando techos de masa térmica. [Tesisi Maestrìa] Universidad Autònoma de Querètaro. https://ri-ng.uaq.mx/handle/123456789/1162

Li, B., & Zhai, X. (2017). Experimental investigation and theoretical analysis on a mid-temperature solar collector/storage system with composite PCM. *Applied Thermal Engineering*, 124, 34–43. https://doi.org/10.1016/j.applthermaleng.2017.06.002

Li, B., Zhai, X., & Cheng, X. (2018). Experimental and numerical investigation of a solar collector/storage system with composite phase change materials. *Solar Energy,* 164, 65–76. https://doi.org/10.1016/j.solener.2018.02.031

Li, C., Zhang, B., Xie, B., Zhao, X., Chen, J., Chen, Z., & Long, Y. (2019). Stearic acid/expanded graphite as a composite phase change thermal energy storage material for tankless solar water heater. *Sustainable Cities and Society*, 44, 458–464. https://doi.org/10.1016/J.SCS.2018.10.041

Li, T., Liu, Q., Liu, L., Li, Y., Yu, J., Wang, X., & Mao, Q. (2023). Feasibility study on solar coupled gas-fired boiler heating system retrofit in residential buildings in the HSCW zone of China. *Case Studies in Thermal Engineering,* 42. https://doi.org/10.1016/j.csite.2023.102698

Luo, X., Hou, Q., Wang, Y., Xin, D., Gao, H., Zhao, M., & Gu, Z. (2017). Experimental on a novel solar energy heating system for residential buildings in cold zone of China. *Procedia Engineering,* 205, 3061–3066. https://doi.org/10.1016/j.proeng.2017.10.282

Maka, A. O. M., & Alabid, J. M. (2022). Solar energy technology and its roles in sustainable development. *Clean Energy,* 6(3), 476–483. https://doi.org/10.1093/ce/zkac023

Martínez Gómez, J., & Argüello Bravo, D. A. (2020). Colector solar térmico, con aire de superficie plana para calefacción y ventilación de áreas internas en viviendas y edificios. Universidad Internacional SEK. http://repositorio.uisek.edu.ec/handle/123456789/3740

Mealla Sánchez, Luis Enrique; Bonaveri Arangoa, P. D. (2012). Construction alternatives using low-cost materials for the thermal test of box-type solar cookers. *Revista ION,* 25(1). http://www.scielo.org.co/scielo.php?script=sci_arttext&pid=S0120-100X2012000100003

Molina Castillo, J. R. (2016). Evaluación bioclimática de una vivienda rural alto andina de la comunidad de San Francisco de Raymina de Ayacucho. Universidad Nacional de Ingeniería. http://hdl.handle.net/20.500.14076/5327

Moscoso Cáceres, M. (2016). Aplicación de los materiales de cambio de fase en el mobiliario interior como reguladores de temperatura (p. 81). Universidad Politècnica de Catalunya. http://hdl.handle.net/2117/102881

Novas, N., Garcia, R. M., Camacho, J. M., & Alcayde, A. (2021). Advances in solar energy towards efficient and sustainable energy. *Sustainability (Switzerland),* 13(11). https://doi.org/10.3390/su13116295

Plytaria, M. T., Tzivanidis, C., Alexopoulos, I., Bellos, E., & Antonopoulos, K. A. (2019). Comparison of two solar-assisted underfloor heating systems with phase change materials. *International Journal of Thermodynamics*, 22(3), 138–147. https://doi.org/10.5541/ijot.495329

Plytaria, M. T., Tzivanidis, C., Bellos, E., & Antonopoulos, K. A. (2018). Energetic investigation of solar assisted heat pump underfloor heating systems with and without phase change materials. *Energy Conversion and Management,* 173, 626–639. https://doi.org/10.1016/j.enconman.2018.08.010

Rabani, M., Bayera Madessa, H., & Nord, N. (2021). Achieving zero-energy building performance with thermal and visual comfort enhancement through optimization of fenestration, envelope, shading device, and energy supply system. *Sustainable Energy Technologies and Assessments,* 44. https://doi.org/10.1016/j.seta.2021.101020

Rahimpour, Z., Faccani, A., Azuatalam, D., Chapman, A., & Verbič, G. (2017). Using Thermal Inertia of Buildings with Phase Change Material for Demand Response. *Energy Procedia*, 121. https://doi.org/10.1016/j.egypro.2017.07.483

Sakhaei, S. A., & Valipour, M. S. (2021). Thermal behavior of a flat plate solar collector with simultaneous use of helically heat collecting tubes and phase change materials. *Sustainable Energy Technologies and Assessments,* 46. https://doi.org/10.1016/j.seta.2021.101279

Sansaniwal, S. K., Mathur, J., & Mathur, S. (2022). Review of practices for human thermal comfort in buildings: present and future perspectives. *International Journal of Ambient Energy*, 43(1), 2097–2123. https://doi.org/10.1080/01430750.2020.1725629

Shabgard, H., Song, L., & Zhu, W. (2018). Heat transfer and exergy analysis of a novel solar-powered integrated heating, cooling, and hot water system with latent heat thermal energy storage. *Energy Conversion and Management,* 175, 121–131. https://doi.org/10.1016/j.enconman.2018.08.105

Shahzad, U., Elheddad, M., Swart, J., Ghosh, S., & Dogan, B. (2023). The role of biomass energy consumption and economic complexity on environmental sustainability in G7 economies. Business Strategy and the Environment, 32(1). https://doi.org/10.1002/bse.3175

Sudhakar, P., & Cheralathan, M. (2021). Encapsulated PCM based double pass solar air heater: A comparative experimental study. *Chemical Engineering Communications*, 208(6), 788–800. https://doi.org/10.1080/00986445.2019.1641701

United Nations. (2015). Transforming Our World: The 2030 Agenda for Sustainable Development. United Nations.

Uribe, D., & Vera, S. (2021). Assessment of the effect of phase change material (PCM) glazing on the energy consumption and indoor comfort of an office in a semiarid climate. *Applied Sciences (Switzerland),* 11(20). https://doi.org/10.3390/app11209597

Wang, D., Liu, H., Liu, Y., Xu, T., Wang, Y., Du, H., Wang, X., & Liu, J. (2019). Frost and High-temperature resistance performance of a novel dual-phase change material flat plate solar collector. *Solar Energy Materials and Solar Cells,* 201. https://doi.org/10.1016/j.solmat.2019.110086

Wang, Z., Diao, Y., Zhao, Y., Chen, C., Liang, L., & Wang, T. (2020). Thermal performance of integrated collector storage solar air heater with evacuated tube and lap joint-type flat micro-heat pipe arrays. *Applied Energy,* 261. https://doi.org/10.1016/j.apenergy.2019.114466

Wang, Z., Diao, Y., Zhao, Y., Wang, T., Liang, L., & Chi, Y. (2018). Experimental investigation of an integrated collector–storage solar air heater based on the lap joint-type flat micro-heat pipe arrays. *Energy,* 160, 924–939. https://doi.org/10.1016/J.ENERGY.2018.07.052

Wang, Z., Diao, Y., Zhao, Y., Yin, L., Chen, C., Liang, L., & Wang, T. (2019). Performance investigation of an integrated collector–storage solar water heater based on lap-joint-type micro-heat pipe arrays. *Applied Thermal Engineering*, 153, 808–827. https://doi.org/10.1016/j.applthermaleng.2019.03.066

Xiao, W., Wang, X., & Zhang, Y. (2009). Analytical optimization of interior PCM for energy storage in a lightweight passive solar room. *Applied Energy,* 86(10), 2013–2018. https://doi.org/10.1016/j.apenergy.2008.12.011

Yu, J., Yang, C., & Tian, L. (2008). Low-energy envelope design of residential building in hot summer and cold winter zone in China. *Energy and Buildings,* 40(8), 1536–1546. https://doi.org/10.1016/j.enbuild.2008.02.020

Zhai, P., Li, J., Lei, T., Zhu, J., & Novakovic, V. (2023). Indoor thermal comfort comparison between passive solar house with active solar heating and without active solar heating in Tibetan. *Energy and Built Environment*. https://doi.org/10.1016/j.enbenv.2023.11.004

Zhang, G., Sun, Y., Wu, C., Yan, X., Zhao, W., & Peng, C. (2023). Low-cost and highly thermally conductive lauric acid–paraffin–expanded graphite multifunctional composite phase change materials for quenching thermal runaway of lithium-ion battery. *Energy Reports,* 9, 2538–2547. https://doi.org/10.1016/J.EGYR.2023.01.102

Zhao, J., Liu, D., & Lu, S. (2022). Research on the Indoor Thermal Environment of Attached Sunspace Passive Solar Heating System Based on Zero-State Response Control Strategy. *Applied Sciences (Switzerland),* 12(2). https://doi.org/10.3390/app12020855

Zhu, Y., Liu, L., Qiu, Y., & Ma, Z. (2022). Design of the passive solar house in Qinba mountain area based on sustainable building technology in winter. *Energy Reports,* 8, 1763–1777. https://doi.org/10.1016/j.egyr.2022.03.026